Modelling and Bayesian adaptive prediction of individual patients' tumour volume change during radiotherapy

Imran Tariq[1], Tao Chen[1,*], Norman F. Kirkby[2], Rajesh Jena[3]

[1] *Department of Chemical and Process Engineering, University of Surrey, Guildford, GU2 7XH, UK*

[2] *Institute of Cancer Sciences, University of Manchester, Manchester, M20 4BX, UK*

[3] *Oncology Centre, Cambridge University Hospitals NHS Foundation Trust, Hills Road, Cambridge, CB2 2QQ, UK*

Abstract

The aim of this study was to develop a mathematical modelling method that can predict individual patients' response to radiotherapy, in terms of tumour volume change during the treatment. The main idea was to start from a population-average model, which is subsequently updated from an individual's tumour volume measurement; therefore the model becomes more and more personalised and so is the prediction. This idea of adaptive prediction was realised by using a Bayesian approach for updating the model parameters. The feasibility of the developed method was demonstrated on the data from 25 non-small cell lung cancer patients treated with helical Tomotherapy, during which tumour volume was measured from daily imaging as part of the image-guided radiotherapy. The method could provide useful information for adaptive treatment planning and dose scheduling based on the patient's personalised response.

Keywords: adaptive radiotherapy, Akaike information criterion, dynamic modelling, intensity modulated radiotherapy, maximum a posteriori estimation, radiobiology.

[*] Corresponding author. Tel.: +44 1483 686593; Email: t.chen@surrey.ac.uk.

1. Introduction

Among available treatments for cancer, radiotherapy has been one of the two most effective methods (the other being surgery) in the care and cure of cancer (Joiner & van der Kogel, 2009). A fundamental task in radiotherapy research is to understand and predict the response of tumour and normal tissues to treatment. This paper is focused on the tumour response; in particular, the modelling and prediction of tumour volume change during the course of radiotherapy. Since tumour volume has been regarded as a measure of treatment response (Bral et al., 2009; Bentzen & Thames, 1996; Dubben et al., 1998; Mozley et al., 2012; Willner et al., 2002), such predictive models could provide useful information that could be used to optimise treatment for individual patients, as demonstrated in computer simulations (Chen et al., 2012; Dionysiou & Stamatakos, 2006; Kim et al., 2009). It should be noted that rapid reduction of tumour volume during radiotherapy can associate with poor outcome (e.g. Brink et al., 2014); therefore care needs to be taken when using volume alone as treatment marker.

Monitoring tumour volume change in radiotherapy has recently become easier than before, due to the wide use of image-guided radiotherapy (IGRT), e.g. the megavoltage computed tomography (MVCT) enabled Tomotherapy and cone-beam CT based systems (Burnet et al., 2010; Xing et al., 2006). During the course of IGRT, tumours can be imaged before each fraction of radiation, providing the measurements of tumour volume at multiple time points during treatment, thus timely indication of tumour response for individual patients (Barker et al., 2004; Loo et al., 2011; Woodford et al., 2007). The availability of such data has generated substantial research interest in developing mathematical models that can describe and predict the time-profile of tumour change, in particular for individual patients. This line of research, if successful, would significantly contribute to personalised optimisation of radiotherapy treatment.

Mathematical modelling of tumour growth and response to radiotherapy has been well reported (e.g. Barazzuol et al., 2010; Chvetsov et al., 2008; Huang et al., 2010; Rockne et al., 2009, 2010). Nevertheless, only until recently it has been possible to model tumour volume change at multiple time points during treatment, thanks to the use of IGRT. Examples include radiobiological modelling the dynamics of gross tumour volume (GTV) during radiotherapy of head-and-neck cancer with four cell populations (Chvetsov et al., 2009). Later the modelling approach was adapted to non-small cell lung

cancer (NSCLC) to estimate the cell survival fraction and its correlation with patient survival time (Chvetsov et al., 2014). An empirical regression model was presented by Seibert et al. (2007) for lung cancer (both non-small cell and small cell) treated by helical Tomotherapy. Recently, we reported a radiobiological modelling study for stereotactic ablative radiotherapy (SABR) of NSCLC (Tariq et al., 2015), which emphasised the need for a systems approach to the selection of proper models. However, these studies have been limited to *fitting* the models to clinical data. Because of large inter-patient variability, it is not clear how the models, developed using data from existing patients, can be used to *predict* the tumour volume change of a new patient.

More recently, the concept of adaptive modelling of tumour volume for individual patients has started to emerge. Zhong & Chetty (2014) showed that the parameters of a radiobiological model can be more accurately estimated by using more data of an individual patient; however they did not explore further to demonstrate adaptive prediction of tumour volume. In another study, Brink et al. (2014) reported that when the model was developed by using the tumour volumes from the first 2/3 of the treatment, its prediction of the remaining 1/3 of the treatment was very good; however the model used was not radiobiology-based but an empirical exponential equation.

Against this background, this paper reports a new Bayesian adaptation approach with radiobiological modelling, for predicting individual patient's tumour volume change during conventionally fractionated radiotherapy of NSCLC. The primary idea is described below. First, a radiobiological model is developed from a population of existing patients. Given the various possible modelling options (e.g. whether tumour growth is exponential or logistic, whether tumour cells are homogeneous, etc.), the Akaike information criterion (AIC) reported in our previous study (Tariq et al., 2015) is applied to select a model that gives good trade-off between goodness-of-fit and model complexity (Burnham & Anderson, 2002). Then, when a new patient is about to be treated, his/her volume change will be predicted based on the population-averaged model, because very little is known about how this patient will respond to therapy *a priori*. Subsequently during the treatment, the population model is adapted (updated) when new GTV measurement is available, so that the model becomes more and more "personalised" to the specific patient and thus the prediction becomes more accurate. Model adaptation to incoming, patient-specific data is realised through a Bayesian parameter

estimation method (Gelman et al., 1995), which facilitates a smooth transition from the population-averaged to a patient-specific model. It is worth noting that the model selection step is necessary, because if the model is too complex and has too many parameters, its quick adaptation to a small amount of patient-specific data will be difficult. The usefulness of the proposed method is demonstrated on NSCLC patients undergoing Tomotherapy.

The method explored in this study could be used in a clinical environment to provide timely and in-treatment prediction of tumour response; such information could be useful for personalised optimisation of the treatment schedule. It should be noted that because the model adaption method relies on patient-specific volume measurements during treatment, it may not be suitable for hypofractionated radiotherapy (e.g. SABR) which does not provide sufficient number of measurements.

2. Patients and data

Twenty five patients, treated for NSCLC on the Hi-Art helical Tomotherapy unit at the London Regional Cancer Program, Ontario, Canada, from 2005 to 2007, were used for this study. The patient cohort and data were originally reported in (Woodford et al., 2007) for 17 patients, and were expanded to have 25 patients when made available to this study. Here only brief description of the patients and data is provided; more detailed information can be found in (Woodford et al., 2007).

All patients received cisplatin and vinorelbine as neoadjuvant chemotherapy, finishing treatment 4-6 weeks before the start of radiotherapy. Chemotherapy is not expected to affect relative GTV changes from radiotherapy because all patients were treated using the same regimen. A prescription dose of 60-64 Gy in 2 Gy per fraction was used for patients in this study, all of whom had locally advanced (Stages III-IV) disease. Prior to treatment, CT simulation, treatment planning and delivery quality assurance were performed to ensure proper dose distributions and absolute dose delivery. During treatment, daily MVCT images were acquired for setup verification. The GTVs used in this study were calculated retrospectively based on the MVCTs. Elective nodal radiation was used for some patients, but the nodes were excluded from the GTV; only primary tumour volume was measured for the modelling purpose in this work. Figure 1 illustrates the GTV change with respect to time for all 25 patients; for clarity the data are shown in two plots on the basis of initial volume. The uncertainties of the measured GTVs

were established to be around 4%, see (Chvetsov et al., 2014) for detailed descriptions.

(a)

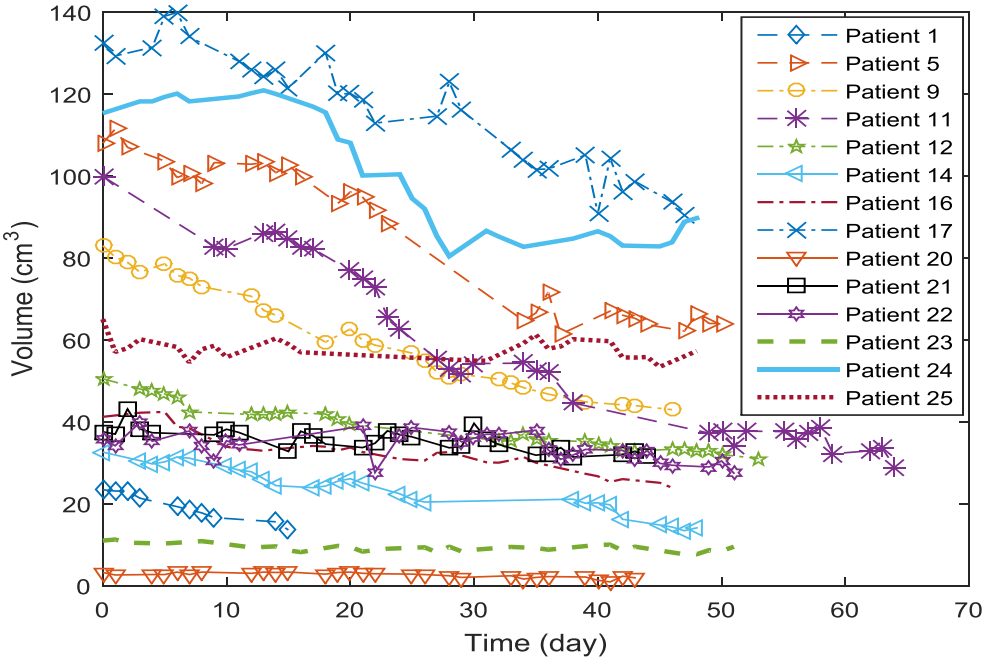

(b)

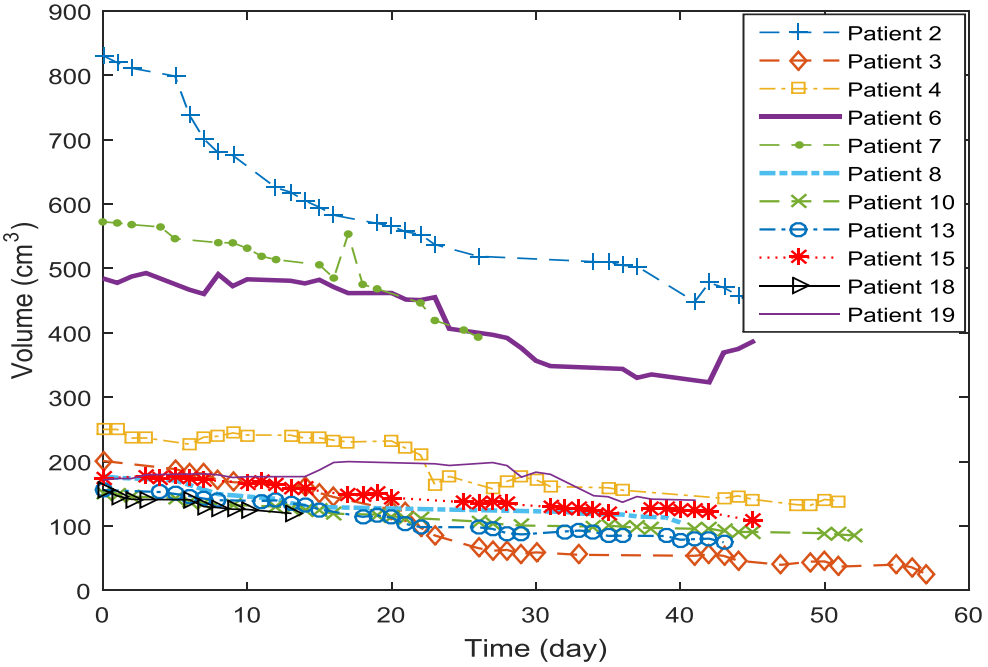

Figure 1. Summary of data used in the modelling study: (a) the initial GTV is less than 150 cm^3; (b) the initial GTV is greater than 150 cm^3.

3. Modelling and Bayesian adaption methods

This section briefly presents the mathematical models used to describe the change of GTV over time, and the AIC method for model selection, similar to our previous modelling study for SABR (Tariq et al., 2015) and other related work (Chvetsov et al., 2014). The focus will then be on presenting a Bayesian model adaptation algorithm for prediction.

3.1. The models

The basic model consists of two types of tumour cells: living or dead. Without radiation, the living cells (volume V_l) will proliferate according to rate γ, and the dead cells (volume V_d) will be cleared according to rate c, as follows:

$$\frac{dV_l}{dt} = \gamma V_l \tag{1}$$

$$\frac{dV_d}{dt} = -cV_d \tag{2}$$

where t is time. The radiation damage on tumour cells is modelled by the linear-quadratic equation, which describes the proportion of living cells surviving irradiation:

$$V_l(t + \Delta t) = V_l(t) \exp(-\alpha d - \beta d^2) \tag{3}$$

where Δt denotes the infinitesimal time after radiation delivered at time t, d is the radiation dose per fraction, and α and β are the model parameters. The killed tumour cells will join the population of dead cells as follows:

$$\begin{aligned} V_d(t + \Delta t) &= V_d(t) + V_l(t)[1 - \exp(-\alpha d - \beta d^2)] \\ &= V_d(t) + V_l(t) - V_l(t + \Delta t) \end{aligned} \tag{4}$$

The total measured tumour volume is then $V = V_l + V_d$.

It should be noted that since the dose per fraction is constant (2 Gy), for the given dose d and surviving fraction $\exp(-\alpha d - \beta d^2)$, there will be infinite combinations of α and β that satisfy this equation. As a result, it is not possible to estimate both α and β. In this study, α/β ratio is fixed to 10 Gy, a value widely used for lung tumours (e.g. Jin et al., 2010). This approach is mathematically equivalent to directly estimating the survival fraction as in (Chvetsov et al., 2014).

The model described in eq. (1)-(4) may be simplified in various ways. One possibility is to ignore cell proliferation; it however cannot well describe some patients whose tumour volume increases during the treatment, and thus is not considered in this study. Another approach is to assume a single type of tumour cells, motivated by the fact that CT images do not differentiate dead from living cells, and thus the actual measurement is only the overall volume. Without the dead cell compartment, the model describes the change of volume due to growth:

$$\frac{dV}{dt} = \gamma V \tag{5}$$

and the shrinkage of volume due to radiotherapy:

$$V(t + \Delta t) = V(t) \exp(-\alpha d - \beta d^2) \tag{6}$$

A major shortcoming of this one-compartment model is that the estimated model parameters do not represent the radiobiology of tumour cells; instead they should be interpreted with respect to the change of the volume, within which both living and dead cells exist.

Finally, the basic model can also be made more complex by including other subtleties. One possibility is to use logistic growth, in place of the exponential growth in eq. (1) or eq. (5), for cell proliferation. Without treatment, tumour would grow indefinitely under the exponential proliferation model, whilst described by logistic growth equation it would reach a plateau due to the lack of sufficient nutrients. The logistic growth for living cell proliferation is described by

$$\frac{dV_l}{dt} = \gamma V_l \left(1 - \frac{V_l}{P}\right) \tag{7}$$

where P is the carrying capacity; by dropping the subscript l, the model for one population can be obtained in place of eq. (5).

It is well accepted that small tumours tend to grow nearly exponentially; but when they become sufficiently large, logistic growth is more applicable due to the effect of cell loss and hypoxia. If the volume (V_l) is much smaller than the carrying capacity (P), logistic growth degenerates to exponential growth. However, logistic growth model introduces one extra parameter (P), and whether this provides better model accuracy needs to be investigated in light of data.

Table 1 summarises the four modelling options to be investigated.

Table 1. Modelling options considered in this study. In the abbreviation, prefix denotes either one type ("1") or two types ("2") of tumour cells, and suffix denotes either exponential ("Exp") or logistic ("Logit") growth.

Model abbreviation	Equations	Parameters
1-Exp	Eq. (5)(6)	$\gamma, \alpha\ (\beta = 0.1\alpha)$
1-Logit	Eq. (5)(7)	$\gamma, P, \alpha\ (\beta = 0.1\alpha)$
2-Exp	Eq. (1)-(4)	$\gamma, c, \alpha\ (\beta = 0.1\alpha)$
2-Logit	Eq. (2)-(4),(7)	$\gamma, P, c, \alpha\ (\beta = 0.1\alpha)$

3.2. Model calibration and selection

We follow the previous study of modelling tumour volume during SABR for model calibration and selection (Tariq et al., 2015). Specifically, the models listed in Table 1 are calibrated to each of the 25 patients by estimating the parameters, using the maximum likelihood method which is equivalent to minimising the sum of squared errors between measured GTV and model fitting. Lower and upper bounds were added to constrain the possible range of the parameters, in light of reported literature data, as follows:

- The rate of proliferation for NSCLC, γ (day^{-1}), was reported to be in the range of [0.001, 0.086] (Sharouni et al., 2003), which was used as the bounds in this paper.
- The survival fraction of NSCLC cell lines under 2 Gy was reported to be between 0.164 and 0.922, which is equivalent to a range of [0.0338, 0.7533] for the linear radiobiological parameter, α (Gy^{-1}), by fixing α/β to 10 Gy.
- The carrying capacity, P (cm^3), varies from patient to patient, and so do the bounds. The lower bound was set as the maximum GTV of a particular patient, while the upper bound is 10 times of the lower bound to allow sufficient space for parameter estimation.
- The clearance rate for dead tumour cells, c (day^{-1}), was reported to be 0.0246, 0.0096 and 0.0383 for different tumours (Chvetsov et al., 2008; 2009). Literature data are sparse for this parameter. In order to allow sufficient freedom for parameter estimation, the bounds were

expanded to set as [0.0045, 0.0540].

The percentage root mean squared error (%RMSE) will be reported to assess model goodness-of-fit. Subsequently, the Akaike information criterion (AIC) (Burnham & Anderson, 2002) was used to help select a model that attains a good balance between complexity and goodness-of-fit. The rationale is that if a model is complex with a large number of free parameters, it would fit the data better than a simpler model. However, complex models tend to over-fit the data and do not generalise well to predict unseen measurements. The AIC is given as

$$\mathrm{AIC} = 2k - 2\ln L \tag{8}$$

where k is the number of free parameters, and L is the maximum likelihood achieved in model calibration. The model with the minimum AIC should be chosen.

It should be noted that this study is focused on prediction for individual patients, for which it is critical to ensure that the modelling option selected provides satisfactory results. Therefore, the model parameters were separately estimated for each patient. A population representation of the parameters will be derived from the distribution of the estimated parameter values, as explained in the section below.

3.3. Bayesian adaptive prediction

The main idea of adaptive prediction is to sequentially improve the prediction of a patient's response to therapy by using data collected during the treatment. When a new patient enters the treatment, the response will be predicted based on a population-averaged model and initial GTV. Subsequently during the treatment, the population model is updated using the GTV measurement of this specific patient, so that the model becomes more and more personalised and the prediction becomes more accurate. Model adaptation will be implemented through a Bayesian parameter estimation method (Gelman et al., 1995), which facilitates a smooth transition from the population-averaged to a patient-specific model.

The Bayesian approach synthesises two sources of information about the model parameters. The first is the prior distribution corresponding to the information about population patients in this study. The second is the likelihood function that represents the data of a specific patient. Let $\boldsymbol{\theta}$ be the set of model parameters and $\mathbf{y}$ denote the data of the patient, Bayes theorem results in the following posterior

distribution of the parameters $p(\boldsymbol{\theta}|\mathbf{y})$:

$$p(\boldsymbol{\theta}|\mathbf{y}) \propto p(\boldsymbol{\theta})\, p(\mathbf{y}|\boldsymbol{\theta}) \tag{9}$$

where $p(\boldsymbol{\theta})$ is the prior and $p(\mathbf{y}|\boldsymbol{\theta})$ the likelihood. Model adaptation is thus achieved by searching for the value of parameters $\boldsymbol{\theta}$ that maximises the posterior probability density function given in eq. (9). Subsequently, the updated parameter value is used for predicting the tumour volume change towards the end of treatment.

In eq. (9), the likelihood function is the same as used for model calibration stage. The prior distribution is derived from the parameters estimated in the model calibration stage explained in Section 3.2. There are 25 patients in the study; for each patient to be predicted, the remaining 24 patients form the population. This ensures that the prior distribution does not contain any specific information from the new patient to be predicted. For each of the model parameters, a log-normal distribution is established from the 24 values of the population patients. Log-normal distribution is used because all model parameters are positive (Table 1). The model parameters are assumed independent *a priori* and thus the overall prior distribution is a product of the log-normal distributions of the *k* parameters:

$$p(\boldsymbol{\theta}) = \prod_{i=1}^{k} p(\theta_i) \tag{10}$$

The above method of obtaining population parameter distribution is a two-stage approach, since it estimates the parameter values for individual patients first, prior to combining them into a distribution. The two-stage approach is used in this study, because we need to assess the model goodness-of-fit for individual patient; it was shown to produce similar results when compared with the more rigorous, non-linear mixed-effect approach for obtaining population parameter distribution directly (Hahn et al., 2011).

Arguably, the parameters can be updated by maximising the likelihood function of patient-specific data only, which is a method widely used in the biomedical community (Chen et al., 2012; Noble et al., 2010). However, the Bayesian approach provides a natural combination of information from population and individual. This is especially useful at the initial stage of the treatment, when the patient-specific data is scarce and maximum likelihood may not give a reliable estimate of the parameters. On the other hand, Bayesian estimation will converge to maximum likelihood method when the amount of data tends to infinity anyway.

In the results section, the two adaptive prediction methods, Bayesian and maximum likelihood, will be compared. In addition, these two methods will be further compared with the prior prediction method (i.e. only using prior population model parameters for prediction with no adaption to individual patients), as well as the model fitting results. The intention was that prior prediction established the baseline results against which adaptive prediction can improve, and the fitting results gave the upper limit of the model accuracy.

4. Results

Two sets of results are presented in this section: those for model calibration and selection, and those for adaptive Bayesian prediction.

Table 2 shows the calibration results of the four models, including the estimated parameters, the %RMSE and AIC values. Since the models were calibrated to 25 individual patients, the median and range of the results are reported. In the light of %RMSE, it appears that more complex models have better goodness-of-fit than simple ones, though the improvement is not substantial. Including carrying capacity (thus exponential growth becoming logistic growth) provides very little benefit (RMSE reduced from 8.85% to 8.39% for one-population model, and no change for two-population model), whilst adding a population of dead cells has more appreciable effect. Based on goodness-of-fit, it might be reasonable to choose the 2-Logit model. However, the trend for AIC is different: adding carrying capacity actually results in worse AIC, which increases from 108 (1-Exp) to 109 (1-Logit) for one-population model and from 79 (2-Exp) to 81 (2-Logit) for two-population model. According to the principle of AIC, using logistic growth is not well supported by the data, and 2-Exp is a good choice in terms of the balance between model complexity and goodness-of-fit. Therefore, the subsequent results will be focused on 2-Exp. In addition, the 5.43% RMSE achieved by 2-Exp is close to the uncertainties of the measured GTVs (around 4%).

Table 2. Summary of the model calibration results.

	γ (day^{-1})	α (Gy^{-1})	P (cm^3)	c (day^{-1})	RMSE (%)	AIC
1-Exp						
median	0.0371	0.0338	-	-	8.85	108
range	[0.012, 0.049]	[0.0338, 0.050]	-	-	[2.52,18.61]	[-38,243]
1-Logit						
median	0.0371	0.0338	899	-	8.39	109
range	[0.001, 0.086]	[0.0338, 0.040]	[18, 1200]	-	[2.51,18.61]	[-36,274]
2-Exp						
median	0.0016	0.4924	-	0.0155	5.43	79
range	[0.001, 0.086]	[0.0338, 0.753]	-	[0.0045, 0.041]	[2.42,14.35]	[-51,245]
2-Logit						
median	0.0016	0.4079	100	0.0155	5.43	81
range	[0.001, 0.086]	[0.0338, 0.753]	[50, 1200]	[0.0045, 0.041]	[2.42,14.35]	[-49,247]

Figure 2 presents the overall satisfactory modelling results of 2-Exp, by plotting the fitted GTV against measured values for all 25 patients. As explained before, the model parameters are fitted to individual patients and thus different patients have different values of the parameters. Figures 3-5 demonstrate the profile of GTV dynamics for three representative patients having the lowest (patient 9), median (patient 6) and highest (patient 19) %RMSE. Even for patient 19 with the highest RMSE, the 2-Exp model is still able to follow the main trend.

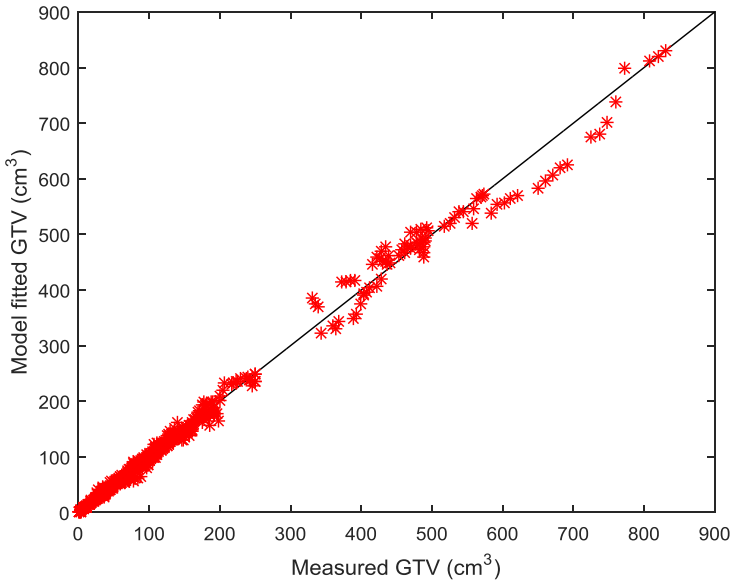

Figure 2. Model fitting results of 2-Exp for all 25 patients' data. The diagonal line corresponds to perfect fit.

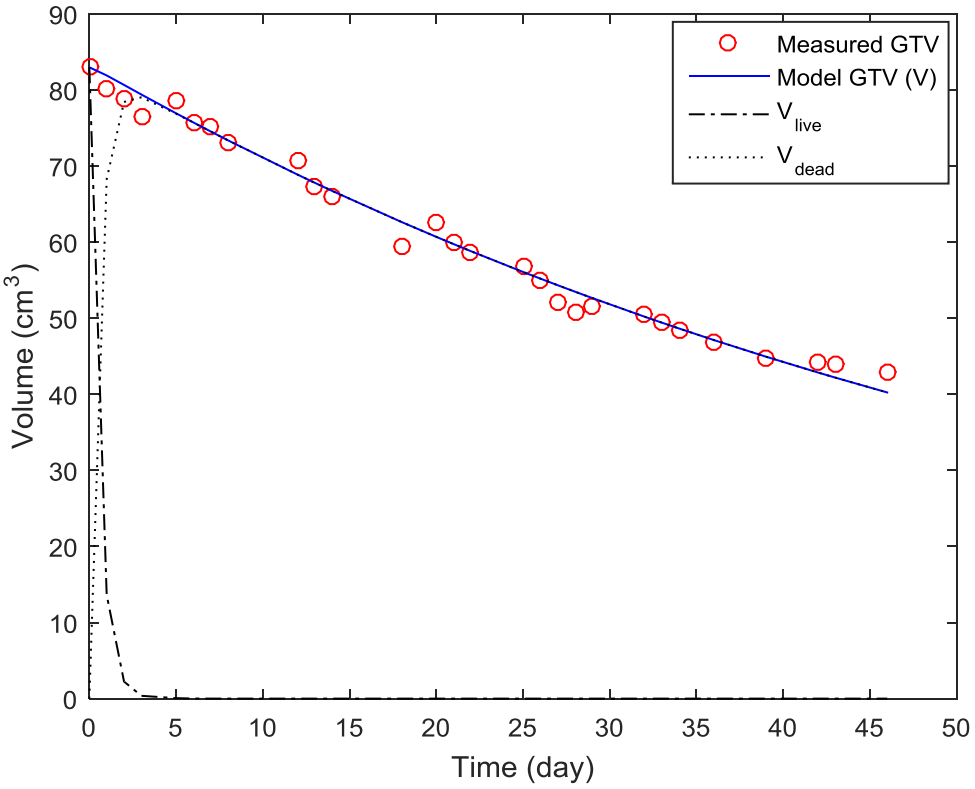

Figure 3. GTV dynamics for patient 9 (RMSE=2.42%).

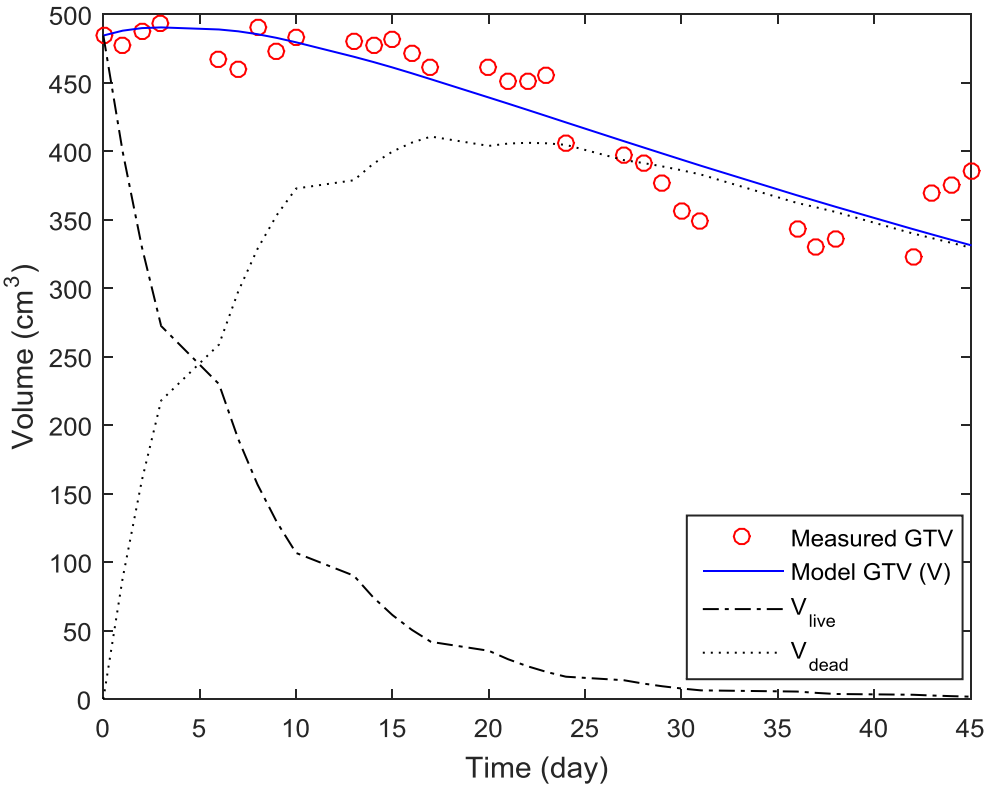

Figure 4. GTV dynamics for patient 6 (RMSE=5.43%).

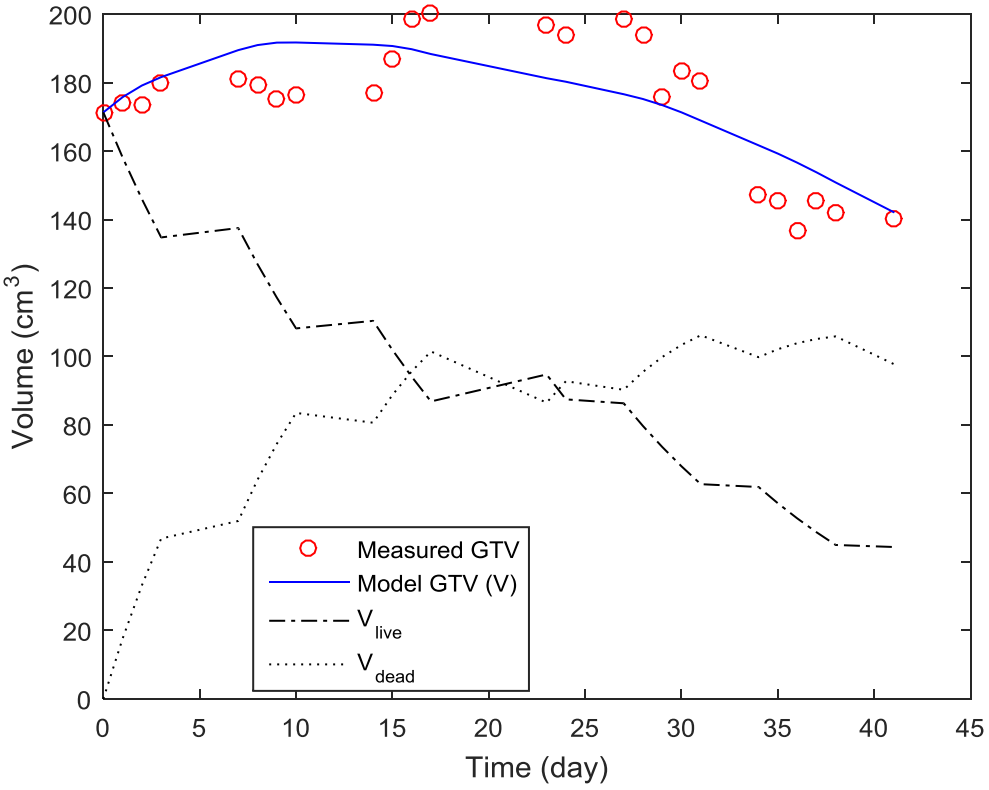

Figure 5. GTV dynamics for patient 19 (RMSE=14.35%).

Next, we present the results of Bayesian adaptive prediction using the 2-Exp model. Note that the prior distribution of the model parameters was assumed to be log-normal. To verify this assumption, Figure 6 gives the histograms of the three parameters as calibrated to the 25 patients individually. As expected, these parameters do not conform to normal distributions, as they must be positive. Instead, Figure 6 shows that log-normal distributions appear to be good representation of γ and c. But for α, almost half of the estimated values are close to the upper bound and thus the distribution appears to be bi-modal. Nevertheless, log-normal distribution was still used for α for its straightforward implementation. The histograms also show a large inter-patient variability for all three parameters estimated.

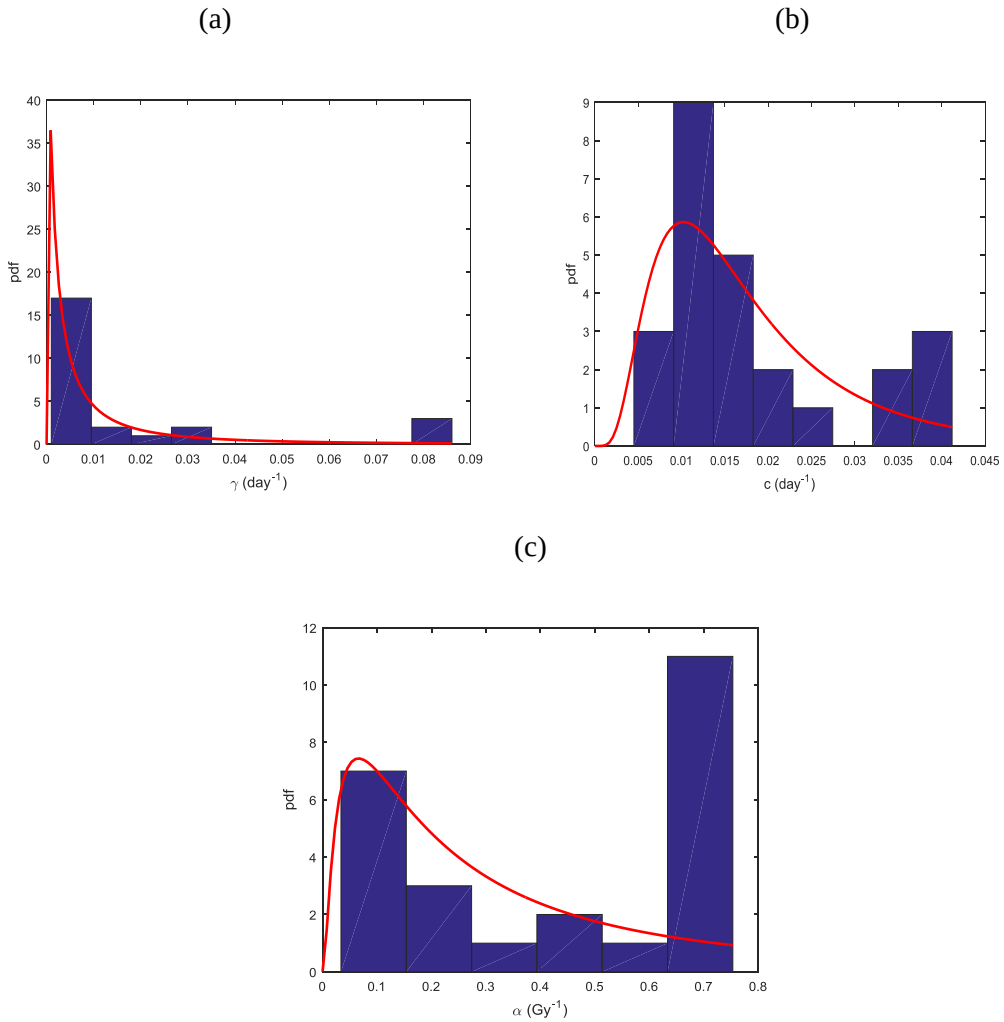

Figure 6. Histograms (normalised to probability density function (pdf)) of estimated parameters for the 2-Exp model, and the fitted log-normal distributions. (a) Rate of proliferation (γ); (b) Rate of clearance (c); (c): The linear killing effect of radiation (α).

Figures 7-9 give the typical results of Bayesian adaptive prediction for three patients, whose model fitting results were shown previously. For clarity, the predicted GTV changes are presented for every five fractions of radiotherapy, though the model and the prediction were actually updated after each fraction of radiotherapy. The prior predictions show similar trend for all patients, since they rely on the similar population parameters which indicate that on average, patients are quite responsive to the treatment with decreasing GTV over time. (Note that the prior distributions are not exactly the same for different patients, because when one patient is to be predicted, it is excluded from the population for calculating the prior. This method is adopted to mimic the reality that a particulate patient's GTV change is not known prior to treatment.) In general, the prior predictions are inaccurate, and for the three patients presented they substantially over-estimate the sensitivity to radiotherapy. The Bayesian adaption method achieved improved prediction to various extent. For patient 9 (Figure 7), the model seems to provide satisfactory prediction as early as fraction 10 (total 28 fractions). However for patient 6 and 19 (Figures 8 and 9, respectively), the computational method could not "foresee" a quick drop of GTV somewhere in the middle of treatment, and thus the predictions were not as satisfactory until late stage of the treatment.

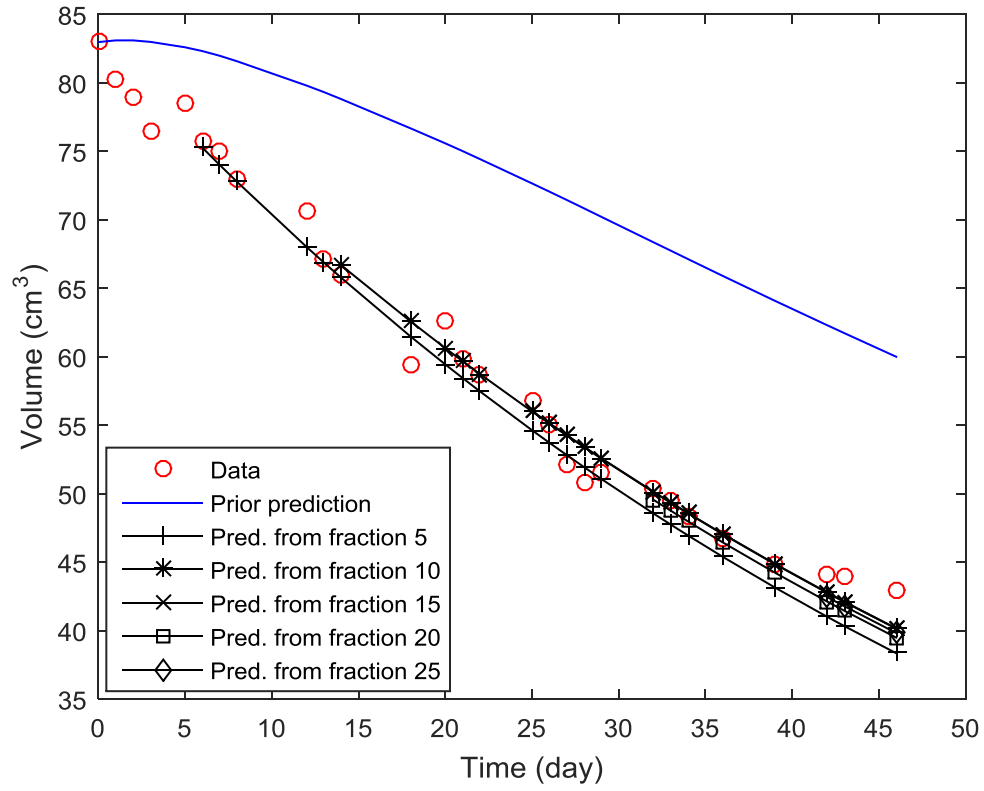

Figure 7. Bayesian model adaptation for patient 9 (the lowest %RMSE in model calibration).

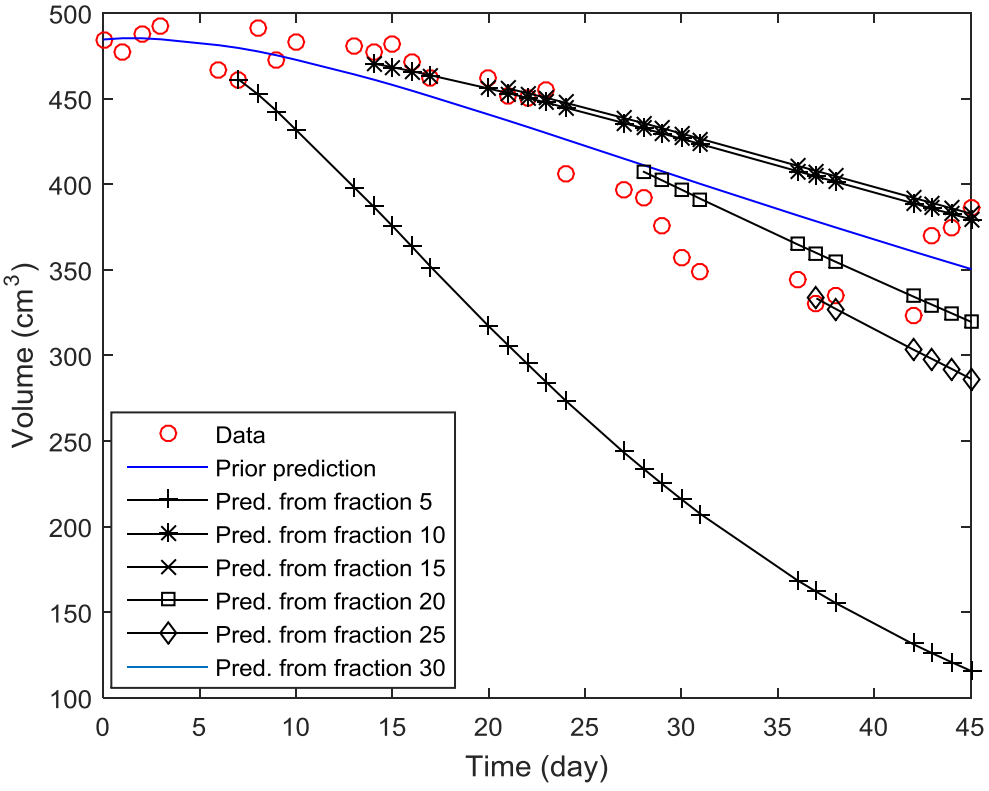

Figure 8. Bayesian model adaptation for patient 6 (the median %RMSE in model calibration).

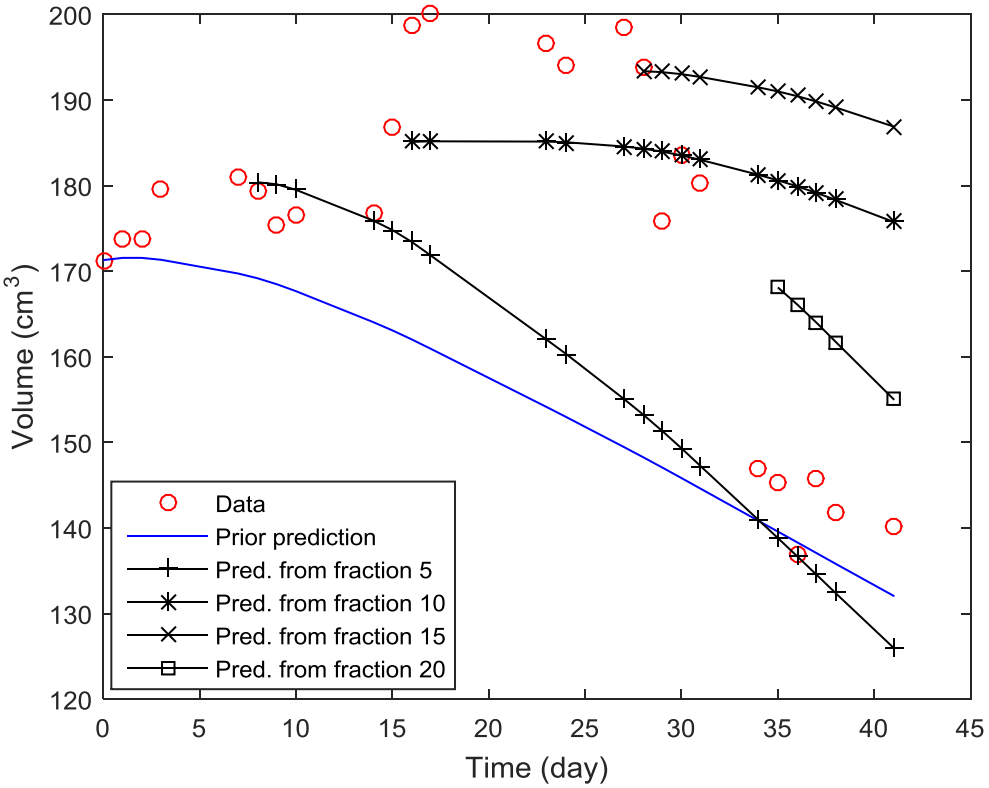

Figure 9. Bayesian model adaptation for patient 19 (the highest %RMSE in model calibration).

Figure 10 summarises the overall prediction results of all 25 patients for Bayesian model adaptation, compared with maximum likelihood (ML) adaptation, prior prediction (i.e. no adaptation), and model fitting (i.e. no prediction). The percentage RMSE is calculated from the time of prediction towards the end of the treatment, which is why the RMSEs for model fitting and prior prediction change slighly with the number of fractions. It can be seen that adaptive prediction methods are useful in terms of reducing errors when compared with prior prediction: this happens after 4 fractions for Bayesian adaption and after 8 fractions for ML adaptation. The improvement in prediction accuracy becomes more apparent when more data are available, e.g. the RMSE at 15 fractions is 30.1% for Bayesian adaptation against 44.2% for prior prediction, and at 20 fractions is 28.0% for Bayesian adaptation against 44.3% for prior prediction. Bayesian method appears to be more reliable than the ML adaptation when the number of fractions, thus the amount of an individual patient's data, is small. When more data become available, Bayesian adaptation converged to the ML method, as expected. Finally, when approaching the last few fractions, adaptive prediction methods achieved an accuracy comparable to

pure model fitting, e.g. at fraction 26, the RMSE for Bayesian adaptation is 13.0% whilst that for model fitting is 11.2%.

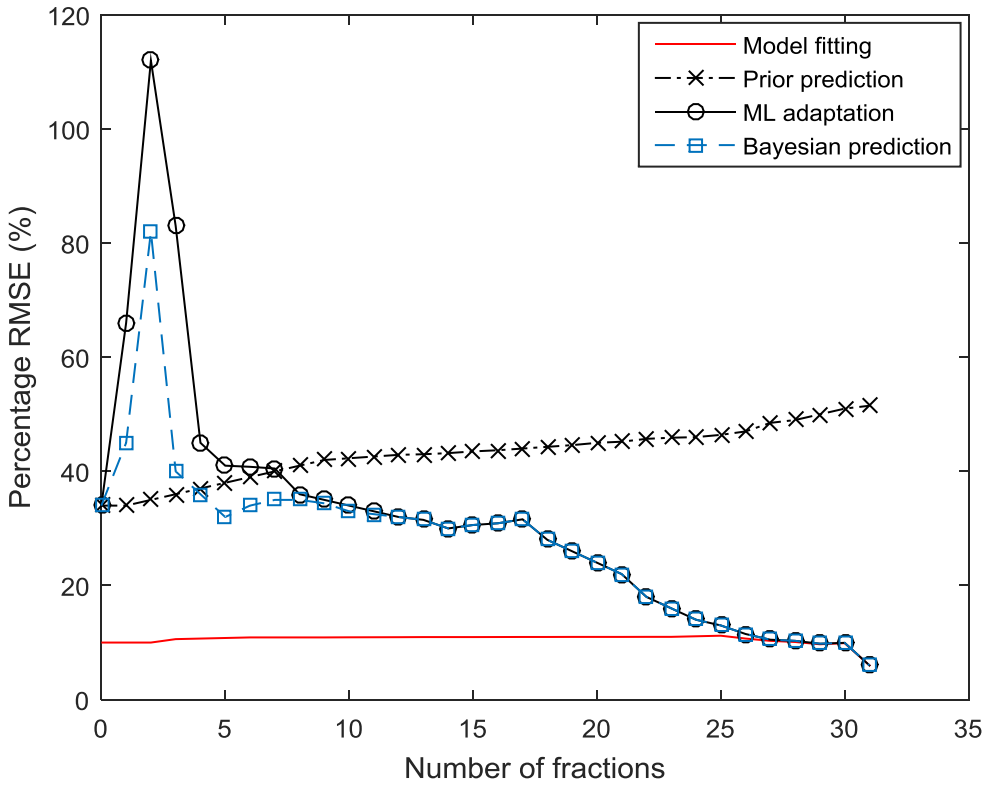

Figure 10. Quantitative analysis of model fitting, Bayesian adaptation, prior prediction and Maximum likelihood adaptation for 25 patient's data

5. Discussions

The first important observation is that the 2-Exp model appears to be a good option for describing tumour volume dynamics in the course of radiotherapy. This model describes the exponential growth of living cells and first-order clearance of dead cells, together with the linear-quadratic equation for the radiation effect. Although tumour cells cannot exponentially grow indefinitely, this model may provide a good balance between model complexity and goodness-of-fit, as assessed by the AIC. It should be noted that similar models have been used in other tumour volume modelling studies (Chvetsov et al., 2014; Tariq et al., 2015).

In addition, the results show substantial variability across different patients, which can be seen

from the wide range of %RMSE and AIC values, as well as the estimated model parameters in Table 2. As expected, different patients may respond to radiotherapy very differently, a phenomenon also observed in our previous report of modelling SABR patients (Tariq et al. 2015), and other related studies (Seibert et al., 2007; Chvetsov et al., 2009; Chvetsov et al., 2014). The inter-patient variability suggests that a population model, which describes some average profile of response to treatment, has limited value in the prediction for individual patients. Patient-specific information is needed for personalised prediction. In this regard, the presented Bayesian adaption approach can adjust the model and prediction based on the patient's early response; it can provide significantly improved prediction as illustrated in Figure 10.

It should be noted that the model adaptation methods (both Bayesian and maximum likelihood) do not give better predictions than the population average at the first few fractions when data are limited. This is expected, since the 2-Exp model has three parameters and cannot be reliably estimated by using, e.g. three data points or less. In other words, the patient has not provided sufficient, individual information for the model to adapt properly. Nevertheless, the Bayesian approach appears to be less susceptible to the limited amount of data when compared with the maximum likelihood method. Therefore, it is recommended that adaptive prediction should only be considered when the number of patient-specific data points is greater than the number of model parameters, and the Bayesian approach is preferred to the maximum likelihood estimation. This requirement may exclude the application of the adaptive prediction method to hypo-fractionation in which only a few fractions of high dose radiation are used (e.g. SABR).

Apparent tumour growth can be observed for some patients, for example patient 19 shown in Figure 9. The same phenomenon was seen in our previous modelling study of hypofrationated radiotherapy (SABR) of lung cancer (Tariq et al., 2015). As discussed in that study, the apparent volume growth could be the result of a number of factors (possibly a combination of them), including (i) actual tumour growth, (ii) tumour inflammatory response to treatment, (iii) surrounding normal tissue's response to treatment, (iv) uncertainties in contouring, and (iv) changes in breathing patter or patient motion. Only the first factor was explicitly represented in the model, since it is not possible to distinguish these from MVCT images.

A limitation of the model adaption approach is its reliance on the data obtained during treatment. If a particular patient's response is very different from the average profile of the population, the prediction will need much more data to be adapted properly. The limitation is vividly illustrated on patient 19, whose GTV only began to reduce from day 30 (Figure 9). Therefore, it is almost impossible to predict that patient 19's GTV will eventually shrink only by looking at the data prior to day 30. The apparent delay in tumour shrinkage is probably due to other patient-specific factors, which are not reflected in the early stage of the treatment. Therefore, the possibility of sudden GTV change in later stage of the treatment needs to be borne in mind when using the predictions for decision-making. It would be useful to identify, as early into treatment as possible, which patients can be well predicted. From Figures 7-9, it is tempting to hypothesise that (i) if a patient responds early to radiotherapy (patient 9), then very good prediction accuracy can be achieved; and conversely (ii) if a patient does not respond until about half into treatment (patient 6 and 19), then prediction will not be as good. However, this hypothesis does not generalise to all patients in the cohort (results not shown). Nevertheless, given the small patient cohort (25 patients), it is too early to tell whether this hypothesis is valid or not. This phenomenon also indicates that, although model adaptation methods provide improved prediction when compared with using population average, they could be further enhanced by including other patient-specific factors. These should be further investigated.

6. Conclusions

This paper presents an adaptive modelling method for predicting the tumour volume change in response to radiotherapy. In terms of model fitting, the results echo previously reported studies in that relatively simple models are adequate for describing tumour volume dynamics. More importantly, the presented Bayesian adaptation method can substantially improve the prediction results by using patient-specific data that are collected along with the treatment. This work represents a step towards developing quantitative tools to support personalised and adaptive approach to radiotherapy.

Future work is focused on extending the adaptive prediction of tumour volume, which is usually a secondary end-point, to primary treatment end-points such as tumour control probability. In addition, we also plan to explore how other factors, in addition to tumour volume, could be included in the

modelling framework to further improve the prediction accuracy. To this end, advanced functional imaging, for example positron emission tomography-computed tomography (PET-CT), is a promising technique. It is known that tumour control probability is determined by the living tumour cells, which cannot be differentiated from those killed by radiation on volume measurements alone. Tumour heterogeneity seen on functional imaging is likely to provide key information for the prediction of treatment outcome, and this will be explored in future work.

Acknowledgements

This work was supported by the UK Engineering and Physical Sciences Research Council through a Doctoral Training Grant. We are grateful to Dr Slav Yartsev at the London Health Sciences Centre, Ontario, Canada for making the tumour volume data available and the useful discussions on radiobiological modelling.

References

Barazzuol L, Burnet NG, Jena R, Jones B, Jefferies SJ and Kirkby NF, 2010. A mathematical model of brain tumour response to radiotherapy and chemotherapy considering radiobiological aspects. Journal of Theoretical Biology, **262** 553-565

Barker JL, Garden AS, Ang KK, O'Daniel JC, Wang H, Court LE, Morrison WH, Rosenthal D, Chao KSC, Tucker SL, Mohan R and Dong L, 2004. Quantification of volumetric and geometric changes occurring during fractionated radiotherapy for head-and-neck cancer using an integrated CT/linear accelerator system. Int. J. of Radiation Oncology, Biol. Phys., **59** 960-970

Bentzen SM, Thames HD, 1996. Tumor volume and local control probability: clinical data and radiobiological interpretations. International Journal of Radiation Oncology Biology Physics, **36** 247-251

Bral S, Duchateau M, De Ridder M, Everaert H, Tournel K, Schallier D, Verellen D, Storme G, 2009. Volumetric response analysis during chemoradiation as predictive tool for optimizing treatment strategy in locally advanced unresectable NSCLC. Radiotherapy and Oncology, **91** 438-442

Brink C, Bernchou U, Bertelsen A, Hansen O, Schytte T, Bentzen SM 2014 Locoregional control of

non-small cell lung cancer in relation to automated early assessment of tumor regression on cone beam computed tomography. International Journal of Radiation Oncology Biology Physics, **89** 916-923.

Burnet NG, Adams EJ, Fairfoul J, Tudor GSJ, Hoole ACF, Routsis DS, Dean JC, Kirby RD, Cowen M, Russell SG, Rimmer YL, Thomas SJ, 2010. Practical aspects of implementation of helical Tomotherapy for intensity-modulated and image-guided radiotherapy. Clinical Oncology, **22** 294-312

Burnham KP and Anderson DR, 2002. Model Selection and Multimodel Inference: A practical information-theoretic approach, **2nd Edition**. Springer-Verlag, New York, 62-64

Chen T, Kirkby NF and Jena R, 2012. Optimal dosing of cancer chemotherapy using model predictive control and moving horizon state/parameter estimation. Computer Methods and Programs in Biomedicine, **108** 973-983

Chvetsov AV, Palta JJ and Nagata Y, 2008. Time-dependent cell disintegration kinetics in lung tumors after irradiation. Physics in Medicine and Biology, **53** 2413-2423

Chvetsov AV, Dong L, Palta JR, Amdur RJ, 2009. Tumor-volume simulation during radiotherapy for head-and-neck cancer using a four-level cell population model. International Journal of Radiation Oncology Biology Physics, **75** 595-602

Chvetsov AV, Yartsev S, Schwartz JL, Mayr N, 2014. Assessment of interpatient heterogeneity in tumor radiosensitivity for nonsmall cell lung cancer using tumor-volume variation data. Medical Physics, **41** 064101

Dionysiou DD, Stamatakos GS, 2006. Applying a 4D multiscale in vivo tumor growth model to the exploration of radiotherapy scheduling: the effects of weekend treatment gaps and p53 gene status on the response of fast growing solid tumors. Cancer Informatics, **2** 113-121

Dubben HH, Thames HD, Beck-Bornholdt HP, 1998. Tumour volume: a basic and specific response predictor in radiotherapy. Radiotherapy and Oncology, **47** 167-174

Gelman AB, Carlin JS, Stern HS, Rubin DB, 1995. Bayesian Data Analysis, **Chapman & Hall/CRC**, Boca Raton, Florida

Hahn JO, Khosravi S, Dumont GA, Ansermino JM, 2011. Two-stage vs mixed-effect approach to

pharmacodynamics modeling of propofol in children using state entropy. Pediatric Anesthesia, **21** 691-698

Huang Z, Mayr NA, Yuh WT, Lo SS, Montebello JF, Grecula JC, Lu L, Li K, Zhang H, Gupta N and Wang JZ, 2010. Predicting outcomes in cervical cancer: a kinetic model of tumor regression during radiation therapy. Cancer Research, **70** 463-470

Jin JY, Kong FM, Chetty IJ, Ajlouni M, Ryu S, Haken RT, Movsas B, 2010. Impact of fraction size on lung radiation toxicity: Hypofractionation may be beneficial in dose escalation of radiotherapy for lung cancers. International Journal of Radiation Oncology Biology Physics, **76** 782-788

Joiner M, van der Kogel A, 2009. Basic Clinical Radiobiology, **4th edition,** Edward Arnold, London

Kim M, Ghate A, Phillips MH, 2009. A Markov decision process approach to temporal modulation of dose fractions in radiation therapy planning. Physics in Medicine and Biology, **54** 4455-4476

Loo H, Fairfoul J, Chakrabarti A, Dean JC, Benson RJ, Jefferies SJ and Burnet NG, 2011. Tumour shrinkage and contour change during radiotherapy increase the dose to organs at risk but not the target volumes for head and neck cancer patients treated on the TomoTherapy HiArt™ system. Clinical Oncology, **23** 40-47

Mozley PD, Bendtsen C, Zhao B, Schwartz LH, Thorn M, Rong Y, Zhang L, Perrone A, Korn R, Buckler AJ, 2012. Measurement of tumor volumes improves RECIST-based response assessments in advanced lung cancer. Translational Oncology, **5** 19-25

Noble S, Sherer E, Hannemann R, Ramkrishna D, Vik T, Rundell A, 2010. Using adaptive model predictive control to customize maintenance therapy chemotherapeutic dosing for childhood acute lymphoblastic leukemia. Journal of Theoretical Biology, **264** 990-1002

Rockne R, Alvord Jr. EC, Rockhill JK, Swanson KR, 2009. A mathematical model for brain tumor response to radiation therapy. Journal of Mathematical Biology, **58** 561–78

Rockne R, Rockhill JK, Mrugala M, Spence AM, Kalet I, Hendrickson K, Lai A, Cloughesy T, Alvord Jr EC, Swanson KR, 2010. Predicting the efficacy of radiotherapy in individual glioblastoma patients in vivo: a mathematical modeling approach. Physics in Medicine and Biology, **55** 3271-3285

Seibert RM, Ramsey CR, Hines JW, Kupelian PA, Langen KM, Meeks SL, Scaperoth DD, 2007. A

model for predicting lung cancer response to therapy. International Journal of Radiation Oncology Biology Physics, **67** 601-609

Tariq I, Humbert-Vidan L, Chen T, South CP, Ezhil V, Kirkby NF, Jena R, Nisbet A, 2015. Mathematical modelling of tumour volume dynamics in response to stereotactic ablative radiotherapy for non-small cell lung cancer. Physics in Medicine and Biology, **60** 3695-3713

Willner J, Baier K, Caragiani E, Tschammler A, Flentje M, 2002. Dose, volume, and tumor control predictions in primary radiotherapy of non-small-cell lung cancer. International Journal of Radiation Oncology Biology Physics, **52** 382-389

Woodford CW, Yartsev S, Dar AR, Bauman G, Van Dyk J, 2007. Adaptive radiotherapy planning on decreasing gross tumor volumes as seen on megavoltage computed tomography images. International Journal of Radiation Oncology Biology Physics, **69** 1316-1322

Xing L, Thorndyke B, Schreibmann E, Yang Y, Li TF, Kim GY, Luxton G, Koong A, 2006. Overview of image-guided radiation therapy. Medical Dosimetry, **31** 91-112

Zhong H, Chetty I 2014. A note on modeling of tumor regression for estimation of radiobiological parameters. Medical Physics, **41** 081702.